

Ambient Air Pressure Effects on Droplet Descent and Dry Surface Impact Dynamics

by

Curtis Evans

B.Eng., University of Victoria, 2006

A Thesis Submitted in Partial Fulfillment of the Requirements for the Degree of

MASTER OF APPLIED SCIENCE

in the Department of Mechanical Engineering

© Curtis Evans, 2024

University of Victoria

All rights reserved. This thesis may not be reproduced in whole or in part, by photocopying or other means, without the permission of the author.

Ambient Air Pressure Effects on Droplet Descent and Dry Surface Impact Dynamics

by

Curtis Evans

B.Eng., University of Victoria, 2006

Supervisory Committee

---

Dr. Peter Oshkai, Supervisor  
(Department of Mechanical Engineering)

Dr. Mohsen Akbari, Department Member  
(Department of Mechanical Engineering)

## ABSTRACT

Droplet impact and the affect of ambient pressure on the droplet impact dynamics are of interest in many applications. These include applications in the industrial, biomedical, environmental and academic fields. When a droplet descends, prior to impact, the ambient pressure, air density and drag forces affect how the droplet behaves in this multi-phase flow. It has been shown that, by reducing ambient pressure, droplet splash can be removed completely [1]. The aim of this study is to perform experiments to further the understanding of that multi-phase flow and gain clarity on how ambient pressure may influence the droplet shape and in-turn, potentially influence the onset of prompt splash upon droplet impact on a dry surface. Instead of reducing ambient pressure to remove splash, this study attempts to increase ambient pressure to induce splash and investigate and compare the droplet dynamics in the pressurized and non-pressurized scenarios using high speed imaging. Conventionally, studies have investigated the droplet upon impact, mostly ignoring the droplet's descent dynamics prior to contacting the dry surface [1] [2] [3] [4]. This study focuses on those pre-impact droplet dynamics by investigating how droplet shapes differ between the pressurized and non-pressurized scenarios. By imaging the droplet descent in a pressurized chamber, a significant difference in the droplet aspect ratio (width-to-height) could be witnessed in the pressurized scenario, compared to the non-pressurized one. The average aspect ratio for droplets descending in an environment with 4atm pressure tended to be greater than 1, deforming droplets to an oblate or elliptical shape. Under standard 1atm pressure, however, droplets under the same velocity conditions tended towards an aspect ratio of 1 (or a spherical shape). Additionally, the amplitude of droplet aspect ratio changes (from oblate to prolate) was higher in the 4atm condition, compared to the 1atm one. As such, it was concluded that when ambient pressure is increased to the point where prompt splash is witnessed, droplet aspect ratio is affected. This may be something to consider when developing a full understanding of the dynamics that affect droplet splash on impact with a dry surface.

# Contents

<b>SUPERVISORY COMMITTEE</b> .....	<b>II</b>
<b>ABSTRACT</b> .....	<b>III</b>
<b>CONTENTS</b> .....	<b>IV</b>
<b>LIST OF TABLES</b> .....	<b>V</b>
<b>LIST OF FIGURES</b> .....	<b>VI</b>
<b>ACKNOWLEDGEMENTS</b> .....	<b>VIII</b>
<b>DEDICATION</b> .....	<b>IX</b>
<b>1 INTRODUCTION</b> .....	<b>1</b>
1.1 RESEARCH CONTEXT AND NOVELTY.....	2
1.2 RESEARCH OBJECTIVES AND METHODOLOGY.....	8
1.3 SIGNIFICANCE AND APPLICATIONS.....	9
1.4 OUTLINE OF THE THESIS.....	10
<b>2 EXPERIMENTAL SYSTEM AND TECHNIQUES</b> .....	<b>11</b>
2.1 GENERAL DESIGN.....	11
2.2 PRESSURE CHAMBER.....	12
2.3 DROPLET DELIVERY.....	14
2.4 CAMERA AND OPTICAL DATA ACQUISITION.....	16
2.5 EXPERIMENTAL PROCEDURE.....	17
<b>3 PRESENTATION AND DISCUSSION OF RESULTS</b> .....	<b>21</b>
3.1 AFFECT OF AMBIENT PRESSURE ON DROPLETS DURING DESCENT.....	22
3.2 AFFECT OF AMBIENT PRESSURE ON DROPLET SPLASH DYNAMICS.....	32
<b>4 CONCLUSIONS</b> .....	<b>34</b>
4.1 SIGNIFICANCE OF FINDINGS.....	35
4.2 FUTURE WORK.....	36
<b>BIBLIOGRAPHY</b> .....	<b>37</b>

## List of Tables

Table 3.1: A table of other experimental studies investigating ambient pressure affects to droplet impacts on a dry surface along with the representative aerodynamic Weber number for their experimental work for droplets splashing compared to not splashing.....	22
Table 3.2: Summary table showing Weber number for each trial location and pressure scenario along with average measured aspect ratios .....	28
Table 3.3: Droplet fluctuations comparison for the two pressure scenarios with droplets travelling at 3m/s as they approach the impact surface, with fluctuations expressed in terms of the average amplitude of deviation from a spherical shape measured in percent of droplet diameter .....	30

## List of Figures

Figure 1.1: Computer generated 3D image of an oblate "hamburger" shaped droplet numerically deformed from the influences of drag forces during droplet decent - Beard et al 2010 .....	7
Figure 2.1: SR-TEK pressure chamber with custom droplet channel modification assembled and ready for pressurization and droplet delivery .....	12
Figure 2.2: Complete experimental apparatus showing high speed camera, lighting, pressure chamber, droplet channel and accompanying tubing and droplet control system .....	13
Figure 2.3: CAD representation of SR-TEK 2000MLCT pressure vessel without any modifications to add the droplet channel to the top of the unit .....	13
Figure 2.4: CAD drawing for custom droplet channel extension with clear acrylic channel for viewing droplet descent .....	14
Figure 2.5: Photograph of droplet being released from release nozzle with droplet necking as critical mass surpasses droplet adhesion forces .....	15
Figure 2.6: Flow chart of the experimental procedure .....	18
Figure 2.7: Basic diagram of droplet pressure chamber and droplet channel with rough height indicated, showing the three primary locations for high-speed video data acquisition of droplets. The boxes drawn along the droplet channel and chamber roughly represent the camera view window for each location.....	20
Figure 3.1: Droplet descent down the droplet channel, after release from nozzle, at location 1 from 0cm to 1.5cm, reaching a velocity of roughly 0.3m/s in the last column of frames for both pressure scenarios. .	23
Figure 3.2: 10 droplet release trials taken at location 1, 1.5cm below the release nozzle, with aspect ratio (width x height) measured for both pressure scenarios.....	24
Figure 3.3: Aspect ratios of droplets under both ambient pressure scenarios measured over 10 trials. at Location 1 (1.5. cm below the nozzle) .....	24
Figure 3.4: Droplet descent down the droplet channel at location 2 from 17.5cm to 19cm, reaching a velocity of roughly 1.9m/s in the last column of frames for both pressure scenarios .....	25
Figure 3.5: 10 droplet release trials taken at location 2, 19cm below the release nozzle, with aspect ratio (width x height) measured for both pressure scenarios .....	25
Figure 3.6: Aspect ratios of droplets under both ambient pressure scenarios measured over 10 trials. at Location 2 (19cm below the nozzle) .....	26
Figure 3.7: Overlay of 10 trials at location 3 (53.6 to 55cm below the nozzle) for both pressure scenarios, reaching a velocity of roughly 3m/s just before impact in the last column of frames .....	27
Figure 3.8: 10 droplet release trials taken at location 3, 55cm below the release nozzle, with aspect ratio (width x height) measured for both pressure scenarios .....	27
Figure 3.9: Aspect ratios of droplets under both ambient pressure scenarios measured over 10 trials. at Location 3 (55cm below the nozzle) .....	28
Figure 3.10: Aspect ratio for 10 droplet heights measured at location 3 from 54.6cm to 55cm for a single droplet trial for both pressure scenarios .....	30
Figure 3.11: Aspect ratios of droplets at 0psi/1atm over 5 trials at location 3, measured at 10 heights between 54.6 and 55cm below the nozzle (i.e. 0 to 13.5mm from impact surface) .....	31
Figure 3.12: Aspect ratios of droplets at 60psi/4atm over 10 trials at location 3, measured at 10 heights between 54.6 and 55cm below the nozzle (i.e. 0 to 13.5mm from impact surface) .....	31
Figure 3.13: A droplet impacting the dry surface at a velocity of roughly 3m/s at 0psi in the left column and 60psi in the right column. An obvious prompt splash can be seen in the pressurized scenario (right column)..	32

Figure 3.14: Droplet impacting the dry surface at a velocity of roughly 3m/s, at 0psi in the left column and 60psi in the right column, with each frame noting a "Yes" or "No" for whether or not a prompt splash (small secondary droplets) are witnessed .....33

## ACKNOWLEDGEMENTS

I would like to thank:

**my parter Ashley Chee and my little boy Ellis Chee-Evans**, for always being there for me and giving me motivation to keep going.

**Dr. Peter Oshkai**, for mentoring, support, encouragement, and patience.

**Fellow team members, Dane Jasek, Zachary Baycroft, Chad Magas and Duncan McIntyre**

for help designing and building the experimental apparatus and providing valuable solutions when I ran into problems.

## DEDICATION

To the hope that this work may have some sort of positive impact to someone.

# Chapter 1

## 1 Introduction

The interaction between liquids and solid surfaces has maintained the attention of researchers across many scientific disciplines. The interplay of forces and behaviors involved in the impact of droplets on surfaces has widespread implications ranging from environmental processes to industrial and biomedical applications. This experimental research endeavors to shed light on a, somewhat, unexplored area in this field—the influence of ambient pressure on the shape of descending droplets and subsequent impact dynamics on dry metal surfaces.

We, the Fluids Research Group under the direction of Prof. Peter Oshkai, at the University of Victoria embarked on an in-depth investigation, aiming to help unravel the intricate relationships between ambient pressure, droplet shape evolution during descent, and impact dynamics. This study aims to provide a significant advancement in the field of fluid-structure interactions, delving beyond conventional analyses that predominantly focused on droplet shape and droplet impacts as mostly standalone phenomena. Through a series of experiments, this research investigates how changes in ambient pressure and air density can significantly impact the shape transformation of a descending droplet of Newtonian fluid, subsequently influencing its impact dynamics upon a dry metal surface.

The dynamics of a descending droplet impacting a dry surface are complex. There is a multitude of factors that are at play that influence the droplet properties as it descends and its subsequent impact on a dry surface. Just a few of these factors include surface tension, ambient air pressure, drag, droplet velocity, droplet size, droplet body oscillations, dry surface roughness, dry surface hydrophobicity (among others).

Varying just one of these factors can greatly change what one might witness with regards to droplet descent behaviour (e.g. droplet shape, oscillation frequency, breakup etc.) as well as the likelihood, mode, and amplitude of a splash when the droplet impacts a dry surface [5].

Since the turn of the last century there have been many publications relating to research in droplet impact dynamics [6], [7]. Worthington, 1908 [8] was one of the first to

investigate these impacts. Using state of the art photography from the day, he was able to capture images of impacting droplets and highlight some of the resultant geometries. Over the last few decades, likely due to technological advances relating to computational fluid dynamics and high-speed photography, the body of work in the research field of droplet impacts has expanded significantly [5]. These technologies have helped to significantly enhance the state of the art in the field by allowing investigation of droplet impact phenomena on a time scale that was previously not possible.

New technologies and resultant research methodologies have allowed for investigation into newly witnessed fluid-structure interaction phenomena. For example and of particular interest to the research presented here, Xu et al, 2005 [1], using high speed photography, were able to demonstrate how ambient pressure could affect the splash of droplets impacting a dry surface. This work was previously not possible, without advances in high-speed photography. Additionally, pressure related affects on droplet impacts was less of a relevant field of study until pressurized fluid-structure interactions became more abundant in industrial and academic processes (e.g. specialized spray coatings and/or high-speed droplet on demand printing).

Since Xu et al, 2005 [1] there have been many studies expanding on the discovery of ambient pressure's influence on droplet splash. This is discussed in more detail below. The work presented in this thesis helps to expand on the current body of research by varying experimental materials (i.e. investigating water) and methods (positive pressure, as opposed to partial vacuum) and presenting a different perspective on potential physical influences on the phenomena (i.e. aerodynamic affects on droplets prior to impact).

## 1.1 Research Context and Novelty

As of the date of this thesis, the majority of work in the field of droplet impacts has largely concentrated on the effects of droplet velocity and material properties on droplet behavior [9] [10] [11] [12], potentially understating the role of ambient air pressure and density in shaping droplet dynamics.

Additionally, past investigations primarily explored the impact of ethanol droplets under reduced ambient pressure conditions [1] [3] [4] [13]. The abundance of water droplets under increased ambient pressure (i.e. water droplets under pressure higher than 1 atm) in nature as

well as other, various, fields of research (discussed further below) imply that there may also be some significant work needed to expand on the existing body of work.

The research presented in this thesis attempts to help in addressing this gap in understanding. This thesis uniquely examines the influence of increased ambient pressure on water droplet behavior during impact. Furthermore, it establishes previously uncharted correlation between droplet descent shape dynamics and the ensuing impact and splash dynamics upon contact with a solid surface.

To bridge this research gap, a review of the existing body of work, relating to general pressure influence on descending and impacting droplets is needed. Previous work can be categorized into their focus on three primary aspects of physical phenomena. These three physical phenomena include: ambient pressure affects on droplets shape as they descend (i.e. how pressure can influence the way droplets shape changes as they move through air), ambient pressure affects on droplets splash after impacting a dry surface (i.e. how pressure can influence the way droplets splash when they impact a dry surface) and affect of droplet shape on splash (i.e. how the shape of a droplet, right before impact, can influence the way the droplet splashes).

### 1.1.1 Pressure Affect on Descending Droplet Shape

With reference to the ideal gas law (as an approximation):

$$P = \rho RT$$

where  $P$  is the pressure,  $\rho$  is the air density,  $R$  is the gas constant and  $T$  is temperature, it is fairly clear to see that the density of air increases proportionally with air pressure. Since the drag force magnitude on an object travelling through air is dependent on the density of air:

$$F_d = \frac{1}{2} \rho V^2 c_d A,$$

where  $V$  is the droplet velocity,  $R_d$  is the drag coefficient for the droplet and  $A$  is the reference area, the drag force on a descending droplet would increase inherently when the air pressure is increased.

E.Loeth, 2006 [11] summarized experimental, theoretical and numerical studies investigating droplets and the affect of drag forces on droplet shape. This review discussed how research showed, as drag increases (by increasing droplet velocity and/or size) the droplet shape transitions to a more oblate shape (i.e. higher W:H aspect ratio) as opposed to a spherical shape (aspect ratio of 1). Additionally, E. Loeth summarized, as drag forces increase, the fluctuations of the droplet shape (i.e. magnitude and frequency of droplet oscillations) tend to increase.

Lin and Palmore, 2022 [14] showed numerically that when ambient pressure on a descending droplet (of a fixed size and velocity) is reduced, drag forces are subsequently reduced and the droplet will tend to a more spherical shape with less magnitude in droplet shape fluctuations.

With this understanding that descending droplet shape changes, based on the aerodynamics influenced by ambient pressure, the question arises “does the evolution of a droplets shape, from its descent influence the dynamics of its splash upon impact with a dry surface?”.

Most of the studies to date, relating to the onset of droplet splashing in reduced ambient pressure, tend to ignore how the droplet shape in their studies (prior to droplet impact) would likely vary significantly in the high pressure cases, compared to the low pressure ones. For example, in 2005, Xu et al were the first to present research showing the absence of splash resulting from a reduction in ambient pressure [1]. However, they did not comment on how the change in aerodynamics during the droplet descent in their trials may have influenced the shape of the droplet as it descended and how that shape change may (or may not) have influenced the dynamics of the droplet splash upon impact.

The research presented in this thesis attempts to show that further consideration of ambient pressure’s affect on droplet shape dynamics (prior to impact) might also be important to consider in the holistic understanding of control parameters governing the occurrence of a droplet splash on a dry surface.

### 1.1.2 Pressure Affect on Droplet Splash on a Dry Surface

A liquid drop hitting a dry surface will often splash, breaking up into many smaller droplets. Due to the complexity of the phenomenon, as described above, the control parameters governing the occurrence of a droplet splash have not been fully explored yet.

Riboux et al, 2014 [15] and Liu et al, 2015 [16] showed that droplet splashing occurs based on the balance between a lift force acting on the liquid and the growth rate of the rim at the edge of the droplet (aka lamella) causing instability and production of secondary “splashing” droplets due to Kelvin-Helmholtz instability. Prior to their work, Mundo et al, 1995 [9] suggested that an empirical model exists to characterize the transition between deposition to splashing using a dimensionless parameter

$$K = OhRe^{1.25} : K > 57.7 = \text{splashing}$$

Here the Reynolds number  $Re$  and the Ohnesorge number  $Oh$  are defined based on droplet properties:

$$Re = \frac{\rho VL}{\mu}, Oh = \frac{\mu}{\sqrt{\rho\sigma L}}$$

where  $\rho$  is droplet density,  $V$  = velocity of the droplet,  $L$  is the characteristic

length of the droplet,  $\mu$  is the viscosity of the droplet and  $\sigma$  is the surface tension.

Mundo et al’s parameter provides a simple method to ascertain the likelihood of a droplet splashing on a dry surface. However, Mundo et al did not consider ambient air pressure (or air density) in their model.

Xu et al, 2005 [1] discovered that ambient air pressure has a significant influence on splashing. In their experiments, they were able to show how splashing can be eliminated on dry surfaces by lowering the surrounding ambient gas pressure.

Many studies followed this discovery in an attempt to broaden the understanding of the phenomenon and help to clarify how ambient pressure might affect the droplet dynamics in a way that can suppress splash upon impact on a dry surface.

Experimentally, in using high speed photography, Latka et al, 2012 [3] confirmed that reduced air pressure also reduces the onset of prompt splash in ethanol. As opposed to the coronal splash originally studied by Xu et al, 2005 [1] and subsequent studies relating to prompt splash [17], prompt splash is the phenomenon where tiny ejecta droplets result from the break-up of the thin droplet lamella almost immediately after impact. Additionally Latka et al, 2012 [3] confirmed the pressure/splash reduction phenomenon is also observed with other liquids by performing experiments with silicone oil.

Numerically (resolving the Navier-Stokes equations and using the moment of fluid method), Guo et al, 2016 [2] confirmed via simulations that reduced ambient air pressure also reduces the onset of droplet lamella break-up (splash) at high speeds ( 50m/s compared to 3m/s by Xu et al). Additionally, their work showed that the pressure/splash reduction phenomenon was not apparent when a droplet impacted a wet surface.

As noted above, Liu et al, 2015 & 2021 [16] [18] attribute splashing to a Kelvin-Helmholtz instability of the gas film under the droplet. Sprittles, 2017 [19] expanded on this and proposes that in the subcontinuum conditions present in the very thin gas film under the droplet a contact line moves faster at reduced ambient gas pressure, causing the gas film to close/collapse earlier at low pressure.

Although many studies have been completed investigating ambient pressure and its influence on droplet splashing, there is still a lack of investigation on how the ambient pressure related shape and dynamics of the droplet during its descent prior to impact (e.g. droplet shape and oscillation fluctuations) may play a role in influencing the likelihood of droplet splash on a dry surface.

Additionally, even though water is abundant in nature and is involved in many of the applications that relate to droplet splash (e.g. rain drops and cooling spray), many studies of the studies noted above do not consider the suppression of water droplet splash (specifically) in reduced ambient pressure conditions [3] [16].

In the research presented in this thesis, water droplets are studied. However, ambient pressure is increased (as opposed to reduced to partial vacuum), allowing the liquid properties of water to be retained and confirm how ambient pressure can also be utilized as a control parameter for water droplet splashes on a dry surface.

### 1.1.3 Droplet Shape Influence on Splash

Liu et al, 2021 [18] showed experimentally that droplet shape, droplet aspect ratio specifically, plays a relatively large role in the onset of droplet splash on a dry surface. When a droplet with a more oblate shape impacts a dry surface the spread velocity of the droplet lamella is greater, compared to a prolate shape. This rapid lamella spreading phenomenon in high aspect ratio (oblate) droplets may be conducive to the onset of prompt splash.

However, the shape of a descending droplet, subject to drag is not simply oblate (i.e. not just an ellipse). Beard et al, 2010 [21] showed, numerically, that the oblate ellipsoidal shape is 3-dimensional and will tend to transition into an oblate ellipsoidal cap at its top, with a dimple on the aft/bottom side. A representation of this can be seen in Figure 1.1 below:

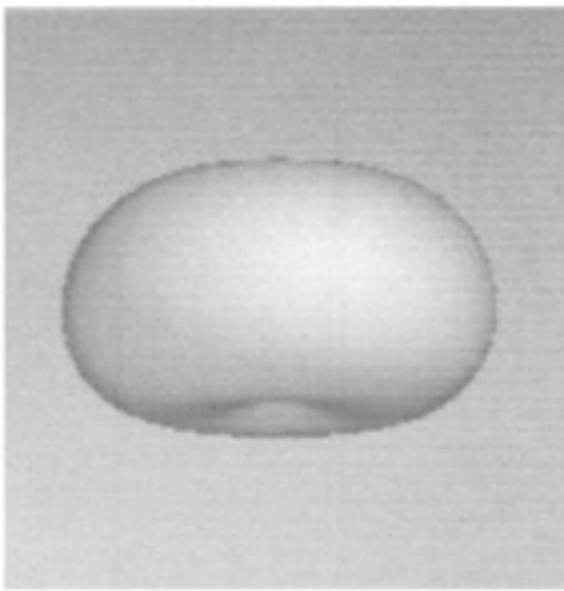


Figure 1.1: Computer generated 3D image of an oblate "hamburger" shaped droplet numerically deformed from the influences of drag forces during droplet decent - Beard et al 2010

Considering how droplets under drag tend towards this shape, one can further hypothesize that, when this droplet shape impacts a dry surface there is higher potential for entrapment of air between the droplet and the dry surface. This has, in fact, been shown in previous experimental and numerical studies by Van der Veen, 2012 [22], Bouwhuis, 2012 [23] and Boelens et al, 2018 [24].

This potential for more air entrapment, when considering the work of Liu et al, 2015 [16] would imply an increase to the Kelvin-Helmholtz instability. Additionally, when referring to the work by Sprittles, 2017 [19] a larger thin film beneath the ellipsoidal dimple droplet shape may yield a greater potential for sufficiently high inertial forces upon impact to produce droplet splash.

#### 1.1.4 Unresolved Issues

In summary, when considering the body of work described above, the main unresolved issue that this thesis intends to help address is whether or not aerodynamic affects on the droplet shape dynamics (prior to impact) may influence droplet splash in high pressure scenarios versus no splash in low pressure scenarios.

Additionally, this work helps to bridge another gap in research where the body of work lacks experimental confirmation of ambient pressure influence on droplet dynamics utilizing water as a fluid material (since most studies use other materials like ethanol [1], silicone oil [3] or ferrofluid [18]) .

### 1.2 Research Objectives and Methodology

This research includes an experimental approach utilizing water as a droplet medium in air. A range of droplet velocities, spanning from 0 to 3 m/s, was examined to ensure a comprehensive understanding of the droplet decent and impact dynamics. Highspeed cameras capable of recording up to 20,000 frames per second were employed to meticulously capture the intricate sequence of events during droplet descent and impact. When describing the conditions of the droplets and comparing one droplet scenario (i.e. ambient pressure, droplet velocity) to another, a scalar value, quantifying each scenario can be used as a helpful way to indicate the physical condition of the droplet in each scenario. Since we will, mainly, be investigating the aerodynamic affects of the air on the droplet as it descends, the aerodynamic Weber number (defined below) is utilized, instead of the standard Weber number, for the presentation of this research.

#### 1.2.1 Droplet Dynamics and Weber Number

The dynamics of descending droplet shape and subsequent break-up and/or splash upon dry surface impact can be described as a fight between the inertial forces acting on the droplet and inter-molecular cohesive forces within the fluid.

When considering a droplet immediately upon impact on a dry surface, the impact force of the surface on the droplet would be in opposition to the viscosity and surface tension of the droplet liquid. As stated above, The Reynolds Number ( $Re$ ), and Ohnesorge ( $Oh$ ) number are dimensionless numbers that are often used as scalar measurements to indicate the ratio between

these inertial forces and cohesive forces. However, another dimensionless number, Weber number, is often used alone as a sufficient dimensionless indicator when examining droplet impact dynamics like spreading, receding, rebounding and splashing [25].

$$We = \frac{\rho V^2 L}{\sigma}$$

where  $\rho$  is the density of the flow field,  $V$  is the droplet velocity and  $\sigma$  is the surface tension. Since the density term represents the density of the flow field, its value is dependent on what inertial flow field is being considered. For example, in the case of a droplet immediately upon impact on a dry surface, the density of the droplet liquid is used to formulate the Weber number. However, if we are considering the aerodynamic drag forces of the ambient gas on the droplet, the density of the air is used. As such, when considering a descending droplet in air, the Weber number is often referred to as the Aerodynamic Weber number [26] [27].

For the most part, in this thesis we will be examining the affect of surrounding air on a droplet as it descends. When noting the Weber number, the Aerodynamic Weber number will be represented when comparing high pressure (high drag) scenarios to low pressure (low drag) ones.

It should also be noted that, within the ranges of ambient pressures examined in this thesis, there will be no significant pressure-induced changes to the inter-molecular cohesive forces of the droplet fluid (i.e. pressure changes will not significantly affect surface tension or viscosity of the liquid or the air) so the surface tension term in the Weber number remains constant [1] [28].

### 1.3 Significance and Applications

The implications of this research expands through a diverse field of sectors, including environmental, industrial, biomedical and academic domains [13]. In industrial applications, insights from this research hold the potential to enhance manufacturing processes involving spray cooling, inkjet printing, and aerosol-based technologies. For biomedical applications, like bioprinting with pressurized cell-laden bioinks, an understanding of droplets surface interactions can help to improve resolution and quality of printing techniques. The elucidation of pressure-dependent droplet impact and splash dynamics can guide the development of optimized techniques for these applications.

In the environmental sphere, a profound understanding of droplet behavior under varied pressure conditions could be pivotal for comprehending natural phenomena such as raindrop impacts on soil or water bodies. Additionally, advancements in the field of fluid-structure interactions facilitated by this research can pave the way for innovations in technologies related to fluid transport, heat exchange, and materials processing [29].

## 1.4 Outline of the Thesis

The following chapters of this thesis delve into the experimental methodology employed, present the empirical results, and offer a comprehensive analysis and discussion of the findings. The subsequent chapters will also highlight the implications of the research in the context of existing literature, substantiating the novelty and significance of the study.

**Chapter 1** contains, in detail, the background of the problems to be investigated, and the impact of pre-existing works to the research and experiments presented in this thesis as well as statement of the claims which will be attempted to be proved by this thesis followed by an overview of the structure of the document itself.

**Chapter 2** describes an approach and methodology for the experiments presented in this thesis along with justification for the methods and processes implemented.

**Chapter 3** is where the results of the experiments are fully described and discussed. It includes the evaluation of the data along with its potential significance when considering pre-existing research in the field.

**Chapter 4** contains a restatement and summarization of the claims and results of the thesis. It also enumerates avenues of future work for further development and/or expansion of the work.

# Chapter 2

## 2 Experimental System and Techniques

The research presented in this thesis is mostly experimental in nature. As such, there was a need to utilize an experimental apparatus that would allow us to physically examine pressure affects to droplet descent and droplet impacts. Since the phenomena related to these affects can often occur in the order of microseconds, experiments of this type are typically carried out with apparatus equipped with high speed cameras [1] [3] [22] [25]. The high temporal resolution of these cameras allows the examiner to obtain visualizations of fluid structure interactions that would not normally be visible to with lower speed visualization methods.

In this research, we utilised a high-speed camera with a capability to obtain images with a temporal resolution suited to these experiments.

### 2.1 General Design

With the help of many members of the Fluids Research Group team, an experimental system was designed and assembled.

A summary of the major components of the system are provided below.

The system included:

- A Photron Fastcam high speed camera, equipped with a Nikon AF Micro Nikkor 60mm 1:2.8 lens capable of up to 20,000 frames per second with a resolution of 256x256.
- A computer system equipped with (camera control hardware and image acquisition software)
- A Nila Boxer, non-flicker, high output light source
- A sealed pressure chamber with a custom-made transparent droplet descent shaft and pre-assembled main chamber impact area, equipped with chamber compatible hosing and adjustable release nozzle height capable of pressures from 0 to 60psi (or 1 to 4atm)
- A droplet delivery system with precise manual servo motor driven fluid driver controlled by button press on custom PLC



Figure 2.1: SR-TEK pressure chamber with custom droplet channel modification assembled and ready for pressurization and droplet delivery

When assembled, the entire system footprint was roughly 1800x900mm in area and was installed within an office room within the Fluids Research Group Lab.

## 2.2 Pressure Chamber

Originally, we considered a custom design and in-house fabrication for a transparent pressure vessel. However, while progressing with preliminary concept development, it was quick to ascertain that the complexity of design, material and precision fabrication requirements were beyond the resources that were allotted to this project. As a result, a pre-made commercial alternative was sought after.

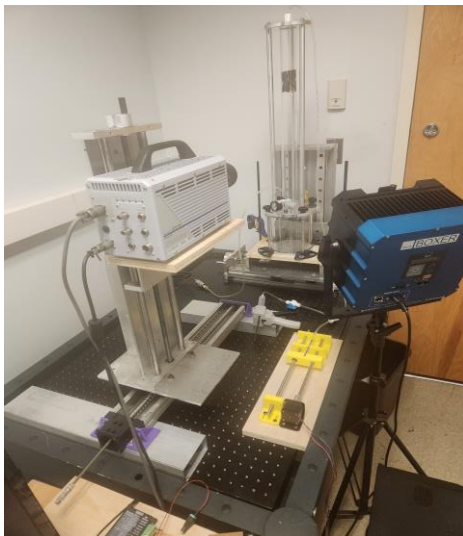


Figure 2.2: Complete experimental apparatus showing high speed camera, lighting, pressure chamber, droplet channel and accompanying tubing and droplet control system

This pressure vessel was the 2000MLCT tank (Figure 2.3) manufactured by SRTEK. These units were designed for precision controlled liquid dispensing, not for use in the academic field. The vessel could only be pressurized safely to 60psi (while we originally were hoping for higher pressures), had a rounded glass transparent body (where a flat body would allow for less potential visualization distortion) and the unit was quite small (only 15cm high - not high enough for gravity driven water droplets to accelerate to adequate velocities to induce splash upon impact).

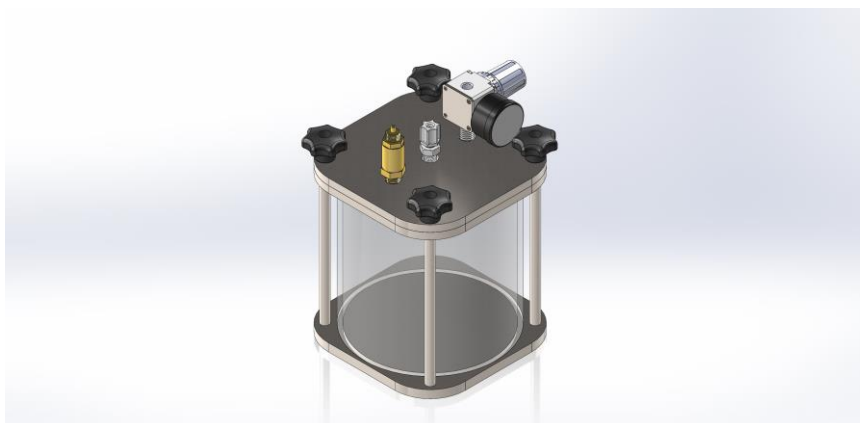


Figure 2.3: CAD representation of SR-TEK 2000MLCT pressure vessel without any modifications to add the droplet channel to the top of the unit

All of the limitations for the commercial unit were acceptable with small changes to the planned experiment process, other than the unit height for adequate droplet delivery velocities. A solution for a custom designed and fabricated extension to be affixed to the SR-TEK unit was developed and implemented (Figure 2.4).

This extension (also referred to as the Droplet Channel) allowed for an adjustable release nozzle (droplet delivery point) height that was capable of providing droplet velocities within the desired range for inducing splash at various vessel pressure intensities.

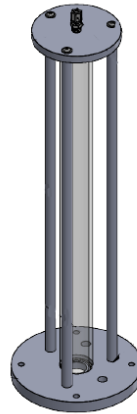


Figure 2.4: CAD drawing for custom droplet channel extension with clear acrylic channel for viewing droplet descent

## 2.3 Droplet Delivery

The droplet delivery mechanism was straightforward. A button-controlled mechanical actuator connected to a syringe with a fluid-filled line that led to the droplet channel and was terminated with a release nozzle where fluid could exit.

When the actuator applied pressure to the syringe incrementally, a corresponding amount of fluid was pushed through the end of the release nozzle. A droplet formed at the end of the release nozzle, held in place by the adhesive forces of the fluid and the release nozzle material. As more fluid was incrementally added to the droplet, the gravitational forces on the droplet surpass the adhesive forces and the droplet was released from the release nozzle to begin its descent down the droplet channel (Figure 2.5).



Figure 2.5: Photograph of droplet being released from release nozzle with droplet necking as critical mass surpasses droplet adhesion forces

One of the limitations of this method, however, is a phenomena where the onset of droplet oscillations occur upon release from the release nozzle. There is a rebound force induced when the neck of the forming droplet releases from the release nozzle [30]. Ideally, a mechanism that delivered a droplet of constant spherical shape would have been utilized. However, implementing a relatively simple mechanism of this sort is a problem yet to be solved in the academic field [31].

The droplet delivery system incorporated 3mm transparent flexible silicone tubing to deliver the fluid to the droplet channel. Transparent tubing was implemented to easily see if any unwanted air pockets or flow obstruction were encountered in the delivery system. A limitation of this tubing material was that it expanded slightly when pressure was applied to the system. This resulted in a gas void forming at the gas/liquid interface upstream of the release nozzle. A supplemental, manual controlled, ratchet syringe system was implemented to rectify this problem and force additional liquid into the system prior to initiating the precision actuator. Another solution would have been to implement glass tubing (or another firm transparent substance), but the costs and design complexity of implementing those materials was considered too great, comparatively.

As noted, water was used as the liquid medium for the experiments presented in this thesis. Water was chosen for four main reasons.

- 1) Water is a freely available and abundant substance.

2) Water is used in a very large cross-section of existing studies relating to the fluid physics that were investigated in this research [5] [15] [9] [20].

3) Water is used in a very large cross-section of industries where this research is applicable (e.g. rain dispersion and spray cooling [32])

4) There is a lack of studies that exist that explicitly investigate the ambient pressure affects on water droplet impacts (as noted above).

## 2.4 Camera and Optical Data Acquisition

There are two predominant phenomena that were investigated in this thesis. They relate to droplet shape oscillation during descent and droplet splash dynamics upon impact.

Both of these phenomena have particular temporal and spatial resolution requirements, when trying to image them. Spatial resolution requirements can, generally, be managed by lensing and magnification. Temporal resolution, on the other hand, often requires more complex imaging hardware.

During descent, droplet shape tends to oscillate from an oblate to prolate shape. Depending on the properties of the droplet (e.g. size, surface tension and liquid density) these oscillations can occur many times per second (on the order of 100Hz). This was originally postulated by Lord Rayleigh, 1879 [10] with the frequency of oscillation being modelled analytically using spherical harmonic modes and a free surface approximation.

Later, an extension to Rayleigh's work to include the affect of ambient fluid and viscous affects was made [33] and many studies followed with further evolution of Rayleigh's hypotheses [30].

Nonetheless, Rayleigh's formulae, still hold up today for simple analysis of many typical droplet descent scenarios [31]. For this thesis and the apparatus employed, there is a capacity to investigate droplets with diameters from 1.5mm to 3mm at velocities up to 4m/s. For a laminar, incompressible flow with constant density and a pure prolate to oblate oscillation of a spheroid with deformations in vertical and horizontal direction the Rayleigh frequency can be reduced to [34]:

$$\omega = \sqrt{\frac{8\sigma}{\rho_{drop} R_{drop}^3}}$$

with radius  $R_{\text{drop}}$ , density drop  $\rho_{\text{drop}}$  and surface tension  $\sigma$ . Using this formula, the maximum oscillation frequency of the droplets potentially investigated would be in the order of about 400Hz. Considering several images would be needed per oscillation to visualize the entire oscillation shape transition, this would require a camera with a shutter speed of at least  $250 \mu\text{s}$  or a video camera capable of at least 4000 frames per second.

However, at a velocity of roughly 4m/s, the onset and disintegration of a droplet splash upon impact can all occur within a fraction of a millisecond (on the order of 0.5 milliseconds) [1]. In order to obtain, at least 10 frames showing this impact/splash transition, imaging with a temporal resolution of at least 5000 frames per second would be required. Higher temporal resolutions were ideal to allow for more frames captured.

For the experiments completed for this thesis, the Photron Fastcam camera met these frame rate requirements (capable of imaging at 20,000 frames per second). As such, many images of the droplet through its descent and subsequent impact could be captured.

The images captured with this camera system were, of course, two dimensional. As such, the three-dimensional shape of the descending droplets and the three-dimensional impact dynamics could not be captured unless multiple cameras were implemented. This, unfortunately, was not an option since multiple cameras were not available and the view angles required were not possible with the apparatus used for the experiments (since the pressure vessel was not fully transparent from all angles). Nonetheless, images sufficient to demonstrate the hypotheses generated in this thesis were adequately obtained.

## 2.5 Experimental Procedure

Prior to imaging (especially the imaging of the droplet impact area), it was important to test and tune the system.

During this process, camera focus, view frame sizing, lighting intensity, ideal pressure settings and ideal release nozzle height were determined.

For the droplet impact scenario, the intent was to show two modes of impact depending on the ambient pressure applied to the system. In the first mode, at lower ambient pressure, the droplet impact would not produce a splash. In the second mode, at higher ambient pressure, the droplet impact would produce a splash. With these two experimental modes, and the only

variation between them being ambient air pressure, it could be clearly shown that changes in ambient air pressure correlate to a significant change in droplet impact dynamics.

Finding the ideal release nozzle height was particularly important during testing and tuning. The relatively small system pressure range (0 to 60psi) was not adequate to induce droplet splash at all droplet velocities. Finding a height to get droplet velocities where no splash occurred at 0psi and a noticeable splash occurred at 60psi was required.

Once the testing and tuning was complete, imaging (data acquisition) could commence. In order to obtain adequate imaging data from the droplet at strategic locations during its descent and impact, two different processes were required. One process was needed for the descent scenario, while another was needed for the impact scenario. The main difference between the two processes was due to the need to dry the impact surface after each image acquisition attempt when investigating the impact scenario. The flow chart (figure 3.10) below shows the process for the droplet impact scenario imaging.

Depending on the type of trial, the experimental process varied significantly with how cumbersome and time consuming it could take. For example, when the system was pressurized and the droplet impact was being investigated, the system had to be decompressed, cleaned, re-pressurized and the droplet line recharged for every trial (as expressed in Figure 2.6).

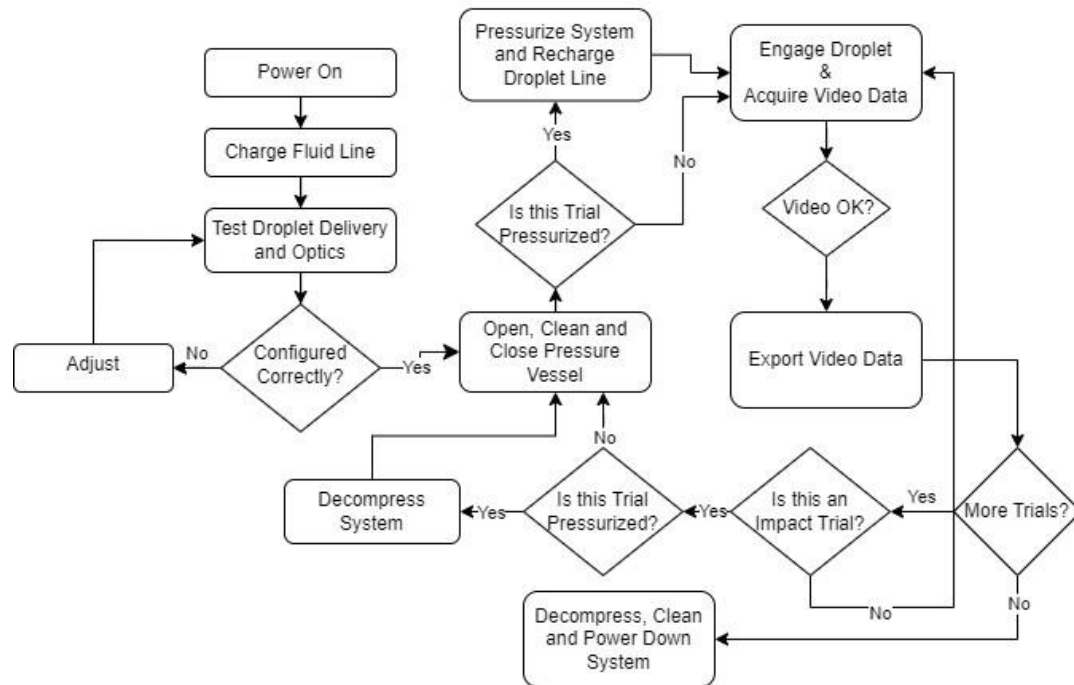


Figure 2.6: Flow chart of the experimental procedure

The outcome of the process described above was a data set that included several sets of short videos (ranging from 300 to 1000 frames) at 20000 frames per second of droplet descent and impact.

It should be noted that, for the purposes of this thesis, a single image at the same location for each scenario and pressure mode would have been sufficient to demonstrate the droplet shape changes. Using the camera in video mode allowed manual triggering of the camera where a single image could later be extracted from the video data. This was deemed as more efficient than designing a highly accurate camera trigger system to ensure the image of the droplet was taken at exactly the same location every time. Additionally, acquiring images in video mode allowed for visual confirmation (by inspecting frames before and after the image to be processed) that the droplets were behaving as expected.

The droplet descent videos were acquired at three locations within the pressurized chamber, as shown in figure (Figure 2.7). Location 1 was immediately below the release nozzle. Location 2 was roughly halfway down the droplet channel. Location 3 was immediately prior to impact with the dry surface. At least 10 videos at each of these locations were obtained for both the 0psi and 60psi (gauge pressure) modes. This resulted in a set of roughly 80 videos that comprised the main data set for the analysis of the droplet descent.

Considering the droplet velocity was highest at location 3, where it would experience the most drag and the ambient air would show a higher influence on the droplet shape (and impact), additional frames of the video were analysed to attempt to gain higher clarity on the phenomenon.

In general, after acquisition of droplet image data at the given locations over multiple sets of trials the images were “processed”. This was done by hand calculating the droplet width and height by measuring the image pixels. This hands-on process produced relatively low error, since the cursor would only slip one or two pixels during measurements while the droplet images were comprised of hundreds of pixels. Considering this, an error analysis was not deemed necessary, as it would not provide additional insight into the results and would not significantly influence the analysis of the data and the conclusions.

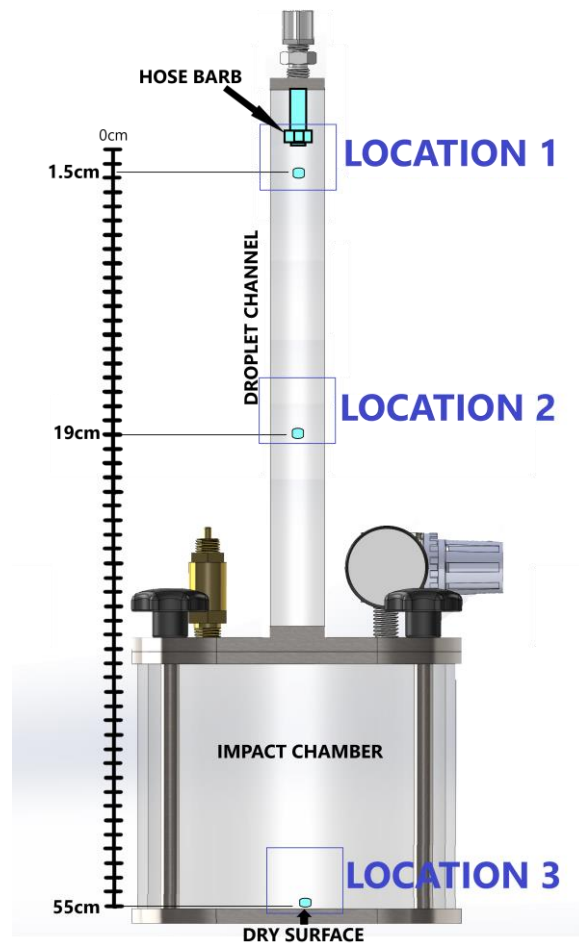


Figure 2.7: Basic diagram of droplet pressure chamber and droplet channel with rough height indicated, showing the three primary locations for high-speed video data acquisition of droplets. The boxes drawn along the droplet channel and chamber roughly represent the camera view window for each location

# Chapter 3

## 3 Presentation and Discussion of Results

Previous experimental studies that investigated ambient pressure effects on droplet impact on a dry surface did not explicitly note the representative aerodynamic Weber numbers of their results [1] [3] [12]. These previous studies tended to concentrate more on the droplet impact than the droplet shape dynamics and aerodynamic drag forces prior to impact. However, we are able to ascertain and calculate what the aerodynamic Weber number would have been, based on the information provided in those studies. Table 3.1 summarizes what the aerodynamic Weber number would have been for the experiments completed in some of these studies for a "splash" and "no splash" condition. We can see that, for the "splash" condition in these studies all of the aerodynamic Weber numbers are greater than 1, where all of the "no splash" conditions show an aerodynamic Weber number of less than 1. Based on this study (and previous studies) [11], these aerodynamic Weber numbers would be representative of relatively large deviations from spherical droplet shapes for the "splash" ( $We > 1$ ) conditions and mostly spherical droplet shapes for the "no splash" condition when predicting the shape of the droplet prior to impacting the dry surface.

As detailed below, our results are in line with expectations, based on previous studies, with regards to droplet shape evolution and splash dynamics upon impact. With our video data broken into frames and aspect ratios of droplets measured at given locations, we can quantitatively and qualitatively compare the droplets in the non-pressurized 0psi and pressurized 60psi (gauge pressure) scenarios. Comparing the aspect ratio of droplets, as they descend and impact the dry surface in the two pressure scenarios, allows us to investigate and evaluate the general affect of the ambient pressure on the basic 2D shape of the droplet.

Author(s)	Year	Droplet diameter (m)	Droplet Velocity (m/s)	Droplet Material	Surface Tension (N/m)	Air Density (High)(Kg/m <sup>3</sup> )	Air Density (Low)(Kg/m <sup>3</sup> )	Splash Weber # ( $\rho \cdot l \cdot V^2 / \sigma$ )	Non-Splash Weber #
L Xu et al	2005	0.0035	3.75	Ethanol	0.0224	1.25	0.175	<b>2.75</b>	<b>0.385</b>
Latka et al	2011	0.0035	3.1	Ethanol	0.0224	1.25	0.1875	<b>1.88</b>	<b>0.282</b>
Latka et al	2011	0.0035	2.7	Silicone Oil	0.0198	1.25	0.375	<b>1.61</b>	<b>0.483</b>
Z Xu et al	2021	0.0035	2	Ethanol	0.0224	2.5	1.25	<b>1.56</b>	<b>0.781</b>

Table 3.1: A table of other experimental studies investigating ambient pressure affects to droplet impacts on a dry surface along with the representative aerodynamic Weber number for their experimental work for droplets splashing compared to not splashing

### 3.1 Affect of Ambient Pressure on Droplets during Descent

Based on previous studies, it was expected that, as the droplets descend at higher velocities and/or higher air density and are subject to higher aerodynamic drag, the Weber number would increase above  $We \gg 1$  and the average shape of the droplets would deviate from the spherical (or 1:1 aspect ratio) shape significantly [11].

The raw data exported from the Photron software was comprised of video files in the avi format. These video files, on average, contained roughly 1000 frames.

Even though the raw data set was captured in a video format, only a single frame from each video was necessary for processing data for the droplet descent scenario. Taking an image at the same locations (labelled location 1, 2 and 3) (Figure 2.7) for each droplet descent trial through the droplet channel allowed us to compare droplet shape from one descent iteration to another, in order to quantify the droplet shape variation in the pressurized (0psi gauge) and non-pressurized (60psi gauge) modes at various droplet heights and subsequent velocities.

#### 3.1.1 Evolution of the Average Droplet Shape

Location 1, as shown in Figure 2.7, represents the area immediately below the release nozzle (where the droplets were released). Data was acquired at this location to assess droplet dynamics during low velocity (and subsequent low Weber number) descent in addition to confirming no significant influence or unexpected phenomena relating to the release mechanism could be witnessed with potential to affect the experimental results.

Below, in Figure 3.1 an indicative selection of frames, showing a droplet trial at 0psi gauge and 60psi gauge as it was released from the release nozzle and began its descent down the channel, can be seen.

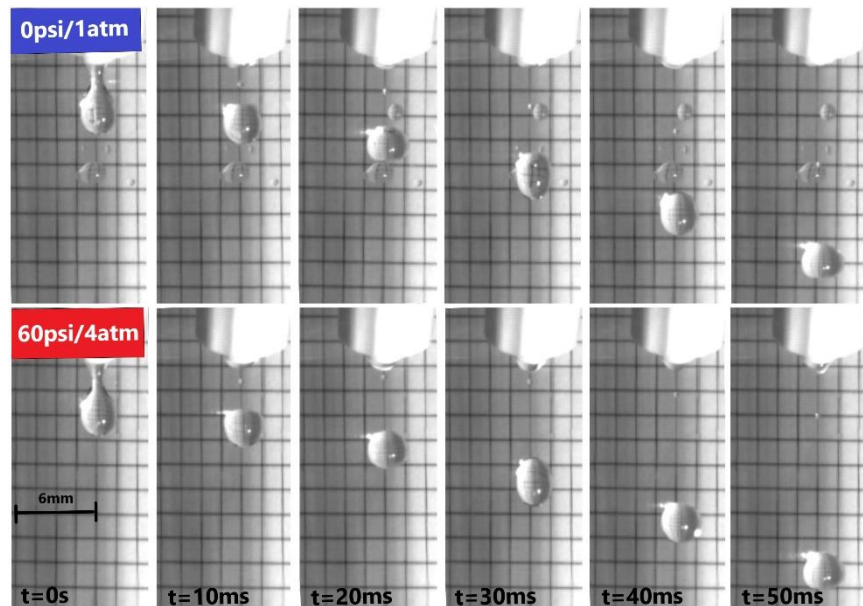


Figure 3.1: Droplet descent down the droplet channel, after release from nozzle, at location 1 from 0cm to 1.5cm, reaching a velocity of roughly 0.3m/s in the last column of frames for both pressure scenarios.

Droplets at location 1, with aspect ratios measured at 1.5cm below the release nozzle (refer to Figure 3.2) and with droplets achieving a velocity of roughly 0.3m/s could be represented by a Weber number of roughly 0.0054 for the 0psi (or air density of  $1.25\text{Kg}/\text{m}^3$ ) scenario and 0.022 for the 60psi scenario.

In both scenarios, the  $We \ll 1$ , so no significant departure from a spherical shape (or an aspect ratio of 1, on average) was expected. Figure 3.3 shows agreement with this expectation highlighting very little deviation from the aspect ratio of 1.

Location 2, as shown in Figure 2.7, represents the area from 15.5cm to 19cm after the nozzle release point. Data was acquired at this location in order to investigate the droplet dynamics at an intermediate velocity, where no significant ambient drag effects were expected from either the 0psi scenario or the 60psi scenario.

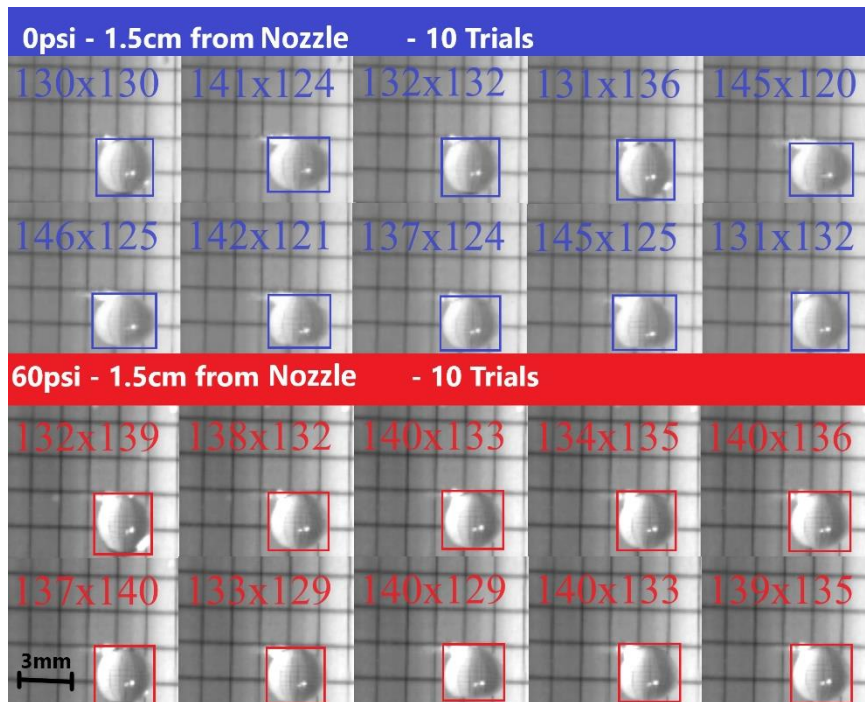


Figure 3.2: 10 droplet release trials taken at location 1, 1.5cm below the release nozzle, with aspect ratio (width x height) measured for both pressure scenarios

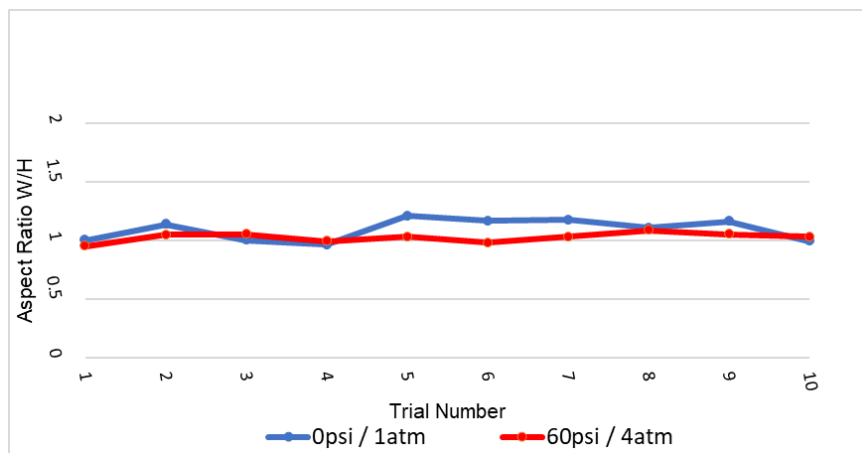


Figure 3.3: Aspect ratios of droplets under both ambient pressure scenarios measured over 10 trials. at Location 1 (1.5. cm below the nozzle)

At location 2, droplets had time to accelerate through their descent to 19cm below the release nozzle achieving a velocity of roughly 1.9m/s (refer to Figure 3.5).

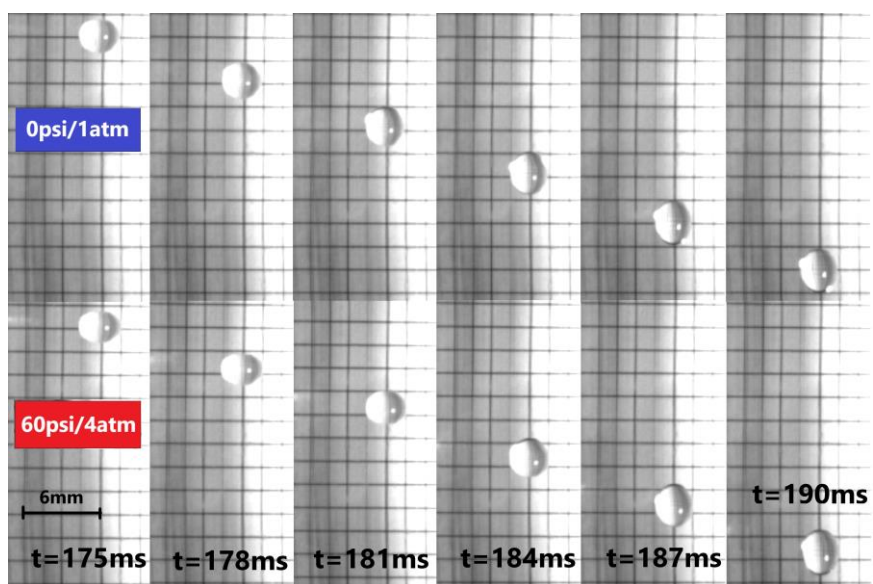


Figure 3.4: Droplet descent down the droplet channel at location 2 from 17.5cm to 19cm, reaching a velocity of roughly 1.9m/s in the last column of frames for both pressure scenarios

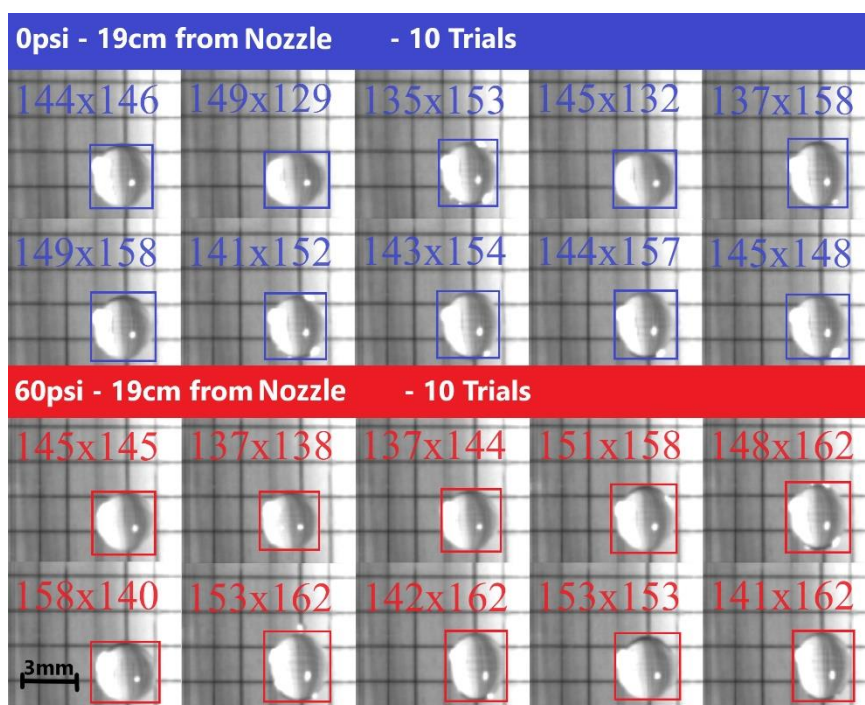


Figure 3.5: 10 droplet release trials taken at location 2, 19cm below the release nozzle, with aspect ratio (width x height) measured for both pressure scenarios

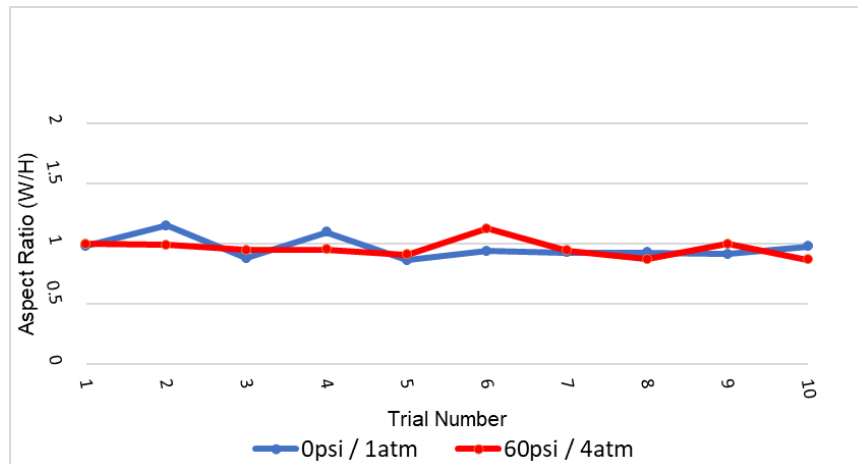


Figure 3.6: Aspect ratios of droplets under both ambient pressure scenarios measured over 10 trials. at Location 2 (19cm below the nozzle)

Velocities of the droplets in both pressure scenarios at location 2 ( $We = 0.22$  for 0psi and  $We = 0.87$  for 60psi) were not adequate to elicit  $We \gg 1$  and also did not show significant deviations from the spherical shape (or an aspect ratio of 1), as shown in Figure 3.6.

Location 3, as shown in Figure 2.7, represents the area from 53.6cm to 55cm after the nozzle release point and includes the dry surface impact zone. Data was acquired at this location in order to investigate the droplet dynamics at higher velocity, where significant ambient drag effects were expected in the 0psi scenario compared to the 60psi scenario. Additionally, data from the impact area could be used to investigate droplet impact dynamics and ascertain whether a splash could be witnessed, or not.

Below, in Figure 3.7 an indicative selection of frames to be processed, showing a droplet trial at location 3 at 0psi and 60psi as it descends down the last cm of the pressure chamber and approaches the impact zone, can be seen.

It was not until we reached the higher droplet velocities (3m/s) at location 3, that we started to expect deviations from a spherical droplet shape in our pressurized scenario (since at 3m/s and 60psi, the Weber number breached the  $We \gg 1$  threshold), on average. The results showed agreement with this expectation (refer to Figure 3.8).

For the 0psi pressure scenario, the representative Weber number could be calculated as 0.54, while the Weber number for the 60psi scenario could be calculated as 2.16. As can be shown quantitatively in Figure 3.9, the 60psi scenario with  $We \gg 1$  shows significant deviation from spherical (i.e. average aspect ratio  $> 1$ ), while the

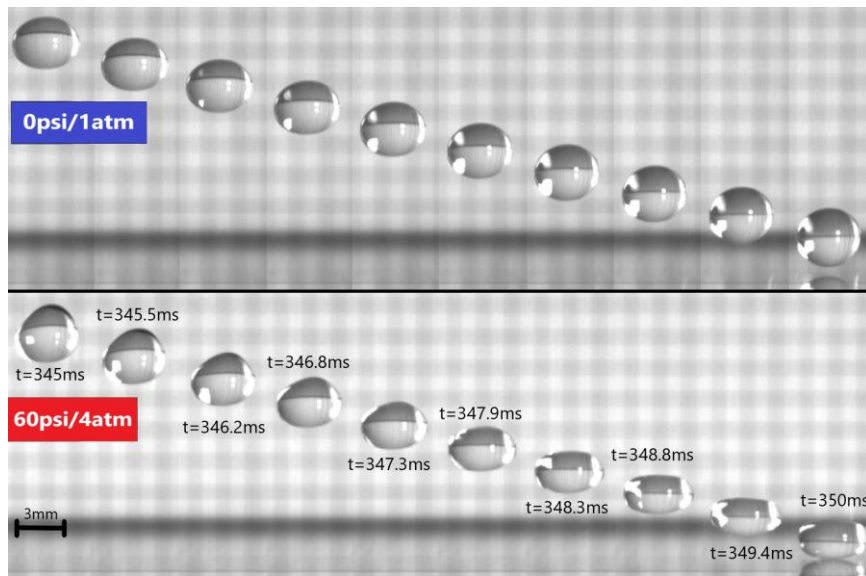


Figure 3.7: Overlay of 10 trials at location 3 (53.6 to 55cm below the nozzle) for both pressure scenarios, reaching a velocity of roughly 3m/s just before impact in the last column of frames

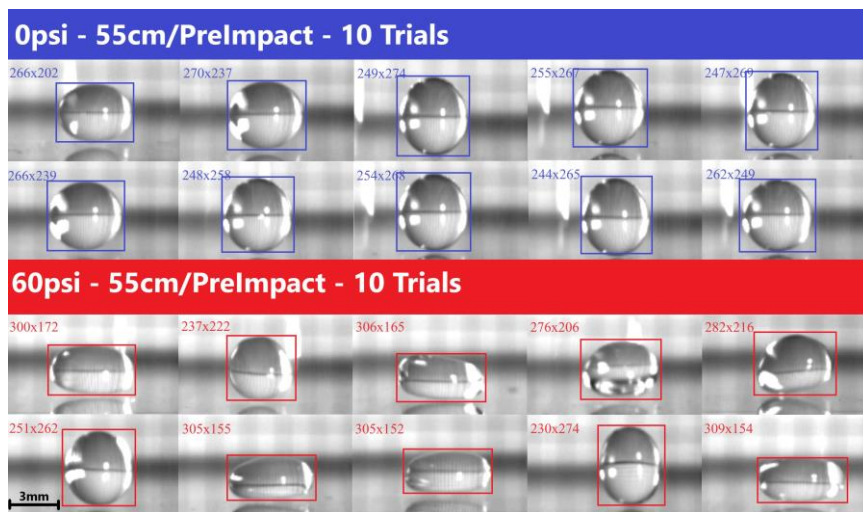


Figure 3.8: 10 droplet release trials taken at location 3, 55cm below the release nozzle, with aspect ratio (width x height) measured for both pressure scenarios

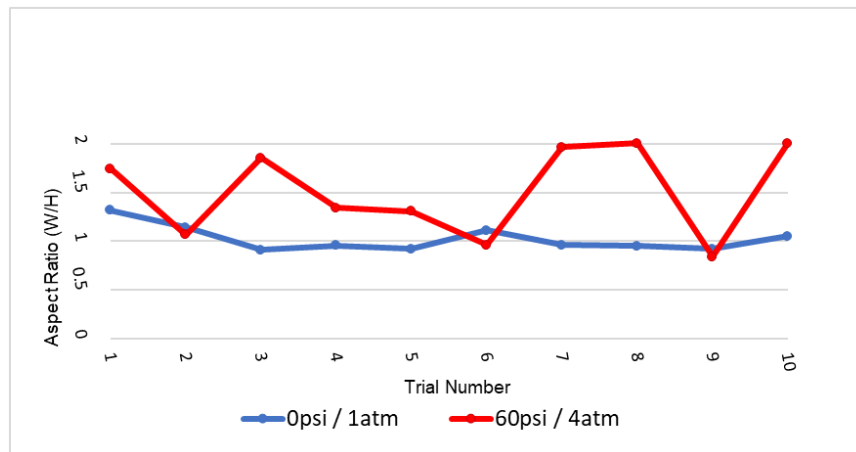


Figure 3.9: Aspect ratios of droplets under both ambient pressure scenarios measured over 10 trials, at Location 3 (55cm below the nozzle)

Trial	Height	Droplet diameter (m)	Droplet Velocity (m/s)	Surface Tension (N/m)	High Air Density (6psi/4atm) (Kg/m <sup>3</sup> )	Low Air Density (0psi/1atm) (Kg/m <sup>3</sup> )	High Air Density Weber #	Average High Air Density Aspect Ratio	Low Air Density Weber #	Average Low Air Density Aspect Ratio	Note:
Location 1	1.5cm	0.0035	0.3	0.0728	5	1.25	<b>0.0216</b>	<b>1.02</b>	<b>0.00541</b>	<b>1.09</b>	No deviation from spherical
Location 2	19cm	0.0035	1.9	0.0728	5	1.25	<b>0.868</b>	<b>0.96</b>	<b>0.217</b>	<b>0.97</b>	No deviation from spherical
Location 3	55cm	0.0035	3	0.0728	5	1.25	<b>2.16</b>	<b>1.51</b>	<b>0.541</b>	<b>1.02</b>	Significant deviation from spherical shape in 60psi/high density trials

Table 3.2: Summary table showing Weber number for each trial location and pressure scenario along with average measured aspect ratios

0psi scenario does not achieve a representative  $We \gg 1$  and does not show significant deviation from spherical (average aspect ratio close to 1).

The representative Weber numbers for all three locations and pressure scenarios along with respective average aspect ratios can be seen in Table 3.2. This table helps to summarize our results along the droplet descent and demonstrates how, as the droplet descends, aerodynamic Weber number increases and the droplet shape evolves from an average spherical shape to an average oblate shape (i.e. average aspect ratio changes from 1 to 1.5).

### 3.1.2 Fluctuations of Droplet Shape

With an increase in air density (and subsequent higher Weber number), there is also an expectation for greater droplet oscillation amplitude [35]. Droplet oscillations can be measured as magnitude and frequency of fluctuations from spherical (or fluctuations in deviation from an aspect ratio of 1). In the experiments presented in this thesis, where a droplet detaches from a

release nozzle and descends (due to gravitational forces exceeding the adhesive forces of the droplet and hosing), droplet oscillations are inherent immediately after release [10]. As the droplet descends after release, it has been shown that, the drag forces (and subsequent Weber number) increase the magnitude of oscillation of the droplet. As the magnitude of oscillation exceeds roughly 10% of the droplet diameter, the frequency of oscillation becomes non-linear and no longer matches the theoretical droplet oscillation frequencies proposed by the Rayleigh droplet oscillation formula [10] [35].

Droplet oscillation frequency wasn't measured explicitly, since it was outside of the scope of this thesis. Aspect ratio, however, was measured and at location 3, where the droplet experienced the highest Weber number, we can see the correlation between increased ambient pressure, subsequent increase in air density and drag and larger fluctuations in the droplet shape.

Considering the highest relative velocity of the droplet occurred just prior to impact, at location 3, video data at this location was also expected to have the highest potential of showing aerodynamic influence on droplet shape. Another, larger data set of video frames were processed at this location, because of this. 10 frames showing droplets as they descend from 53.8cm to 55cm were taken from the video data for 10 different trials at the 0psi and 60psi pressure scenarios. Figure 3.7 shows a representation of the data from one of those trials. Measuring the aspect ratio of the droplets through this range of the descent allowed us to track the amplitude and fluctuations of the droplet shape change with higher temporal resolution (where droplet shape fluctuations is considered the magnitude of aspect ratio changes over a given distance/time).

Figure 3.10 shows aspect ratio of droplets measured for the 10 frames from a single droplet descent trial at the 0psi and 60psi pressure scenarios over the last 1.4cm of droplet descent, where the droplet velocities reached roughly 3m/s.

The 10 droplet aspect ratios measured over the last 1.4cm of the droplet descent were compared for 5 different trials for the 0psi pressure scenario and 10 different trials for the 60psi pressure scenario, which can be seen in Figure 3.11 and Figure 3.12 respectively.

In Figure 3.8 and Figure 3.10 we can qualitatively assess larger fluctuations in droplet shape, with obvious shape changes from prolate to oblate. In Figure 3.9, Figure 3.11 and Figure 3.12 the results are quantified, showing aspect ratios that vary much more for the high pressure (60psi gauge) scenario than the lower pressure (0psi gauge) scenario. Table 3.3 summarizes the

fluctuations in droplet shape based on data from Figure 3.11 and Figure 3.12 highlighting the fluctuation in droplet shape in terms of the % of droplet

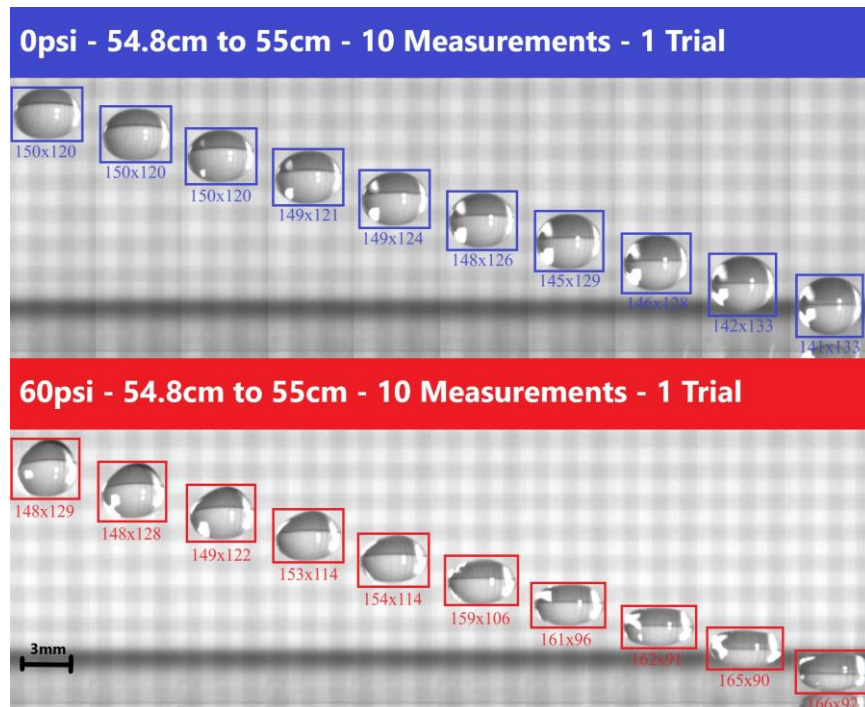


Figure 3.10: Aspect ratio for 10 droplet heights measured at location 3 from 54.6cm to 55cm for a single droplet trial for both pressure scenarios

diameter for each scenario. The results are in line with our expectations, showing high droplet shape fluctuations with higher Weber number. We also can see that fluctuations are greater than 10% of the droplet diameter. This implies that nonlinear affects to droplet oscillation frequency would be expected in the higher Weber number, pressurized, scenario.

Ambient Pressure	Average Aspect Ratio	Standard Deviation	Highest Aspect Ratio	Lowest Aspect Ratio	Average Deviation from Spherical (% diameter)
0psi/1atm	1.02	0.125	1.31	0.91	1.96
60psi/4atm	1.51	0.436	2.01	0.83	33.77

Table 3.3: Droplet fluctuations comparison for the two pressure scenarios with droplets travelling at 3m/s as they approach the impact surface, with fluctuations expressed in terms of the average amplitude of deviation from a spherical shape measured in percent of droplet diameter

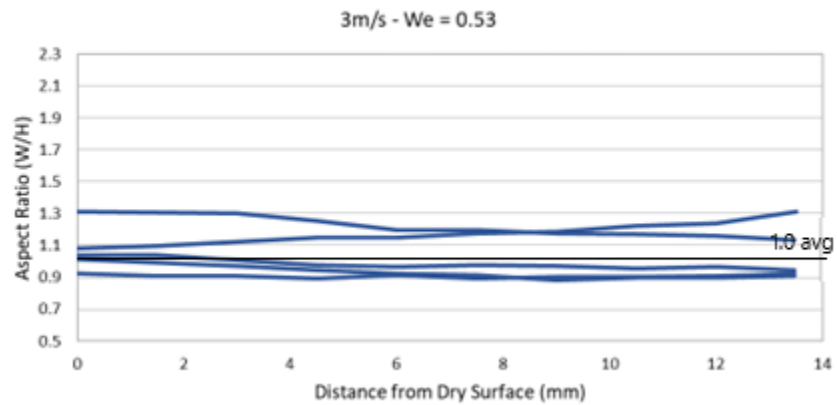


Figure 3.11: Aspect ratios of droplets at Ops/1atm gauge over 5 trials at location 3, measured at 10 heights between 54.6 and 55cm below the nozzle (i.e. 0 to 13.5mm from impact surface)

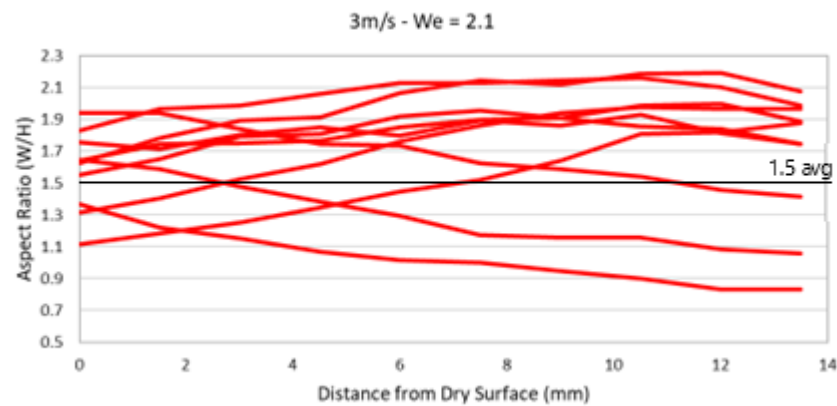


Figure 3.12: Aspect ratios of droplets at 60psi/4atm gauge over 10 trials at location 3, measured at 10 heights between 54.6 and 55cm below the nozzle (i.e. 0 to 13.5mm from impact surface)

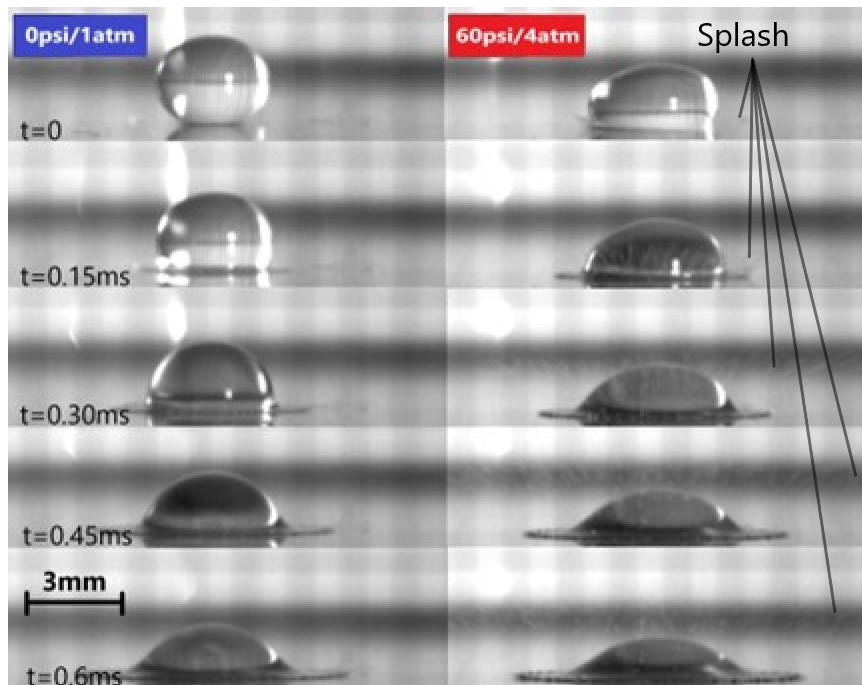


Figure 3.13: A droplet impacting the dry surface at a velocity of roughly 3m/s at 0psi gauge pressure in the left column and 60psi gauge pressure in the right column. An obvious prompt splash can be seen in the pressurized scenario (right column)

## 3.2 Affect of Ambient Pressure on Droplet Splash Dynamics

In Figure 3.13 an indicative selection of frames to be processed, showing a droplet trial at 0psi gauge and 60psi gauge as it impacts the dry surface, can be seen.

Processing of droplet impact scenario data was simply a "yes" or a "no" outcome relating to whether a splash occurred or not. This was done by assessing whether any secondary microdroplets were witnessed in the first 10 frames (at 20,000 fps) following impact.

For all 0psi droplet impact trials there was a "no" outcome. That is, 100 percent of all frames representing droplets impacting at 0psi gauge ambient pressure showed no evidence of splash. For all 60psi droplet impacts there was a "yes" outcome. That is, at least one of the frames in each trial representing droplets impacting at 60psi gauge ambient pressure showed evidence of a splash. As can be seen qualitatively in Figure 3.14, a prompt splash was observed

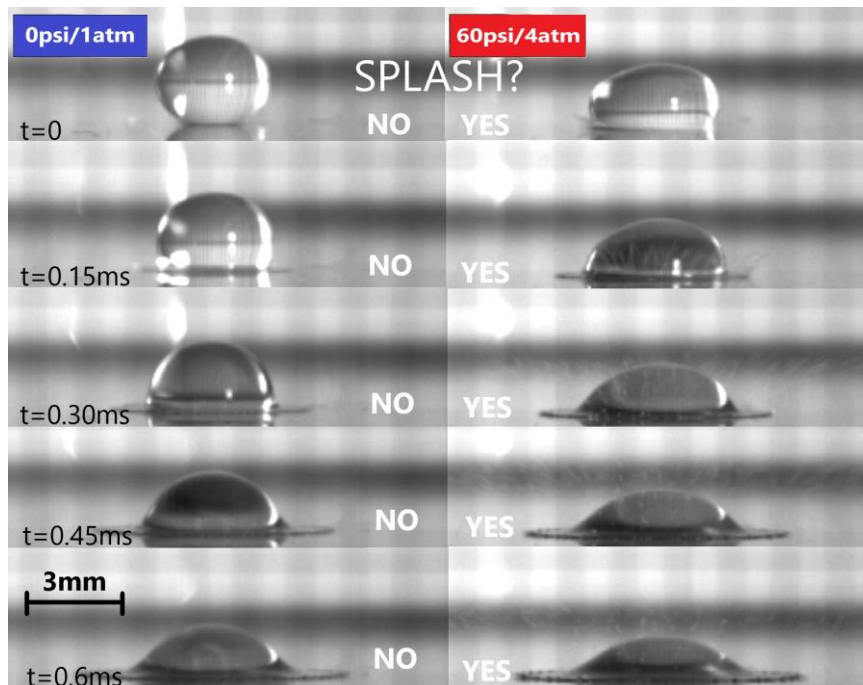


Figure 3.14: Droplet impacting the dry surface at a velocity of roughly 3m/s, at 0psi gauge pressure in the left column and 60psi gauge pressure in the right column, with each frame noting a "Yes" or "No" for whether or not a prompt splash (small secondary droplets) are witnessed

microdroplets observed in frame) in all of the trials performed in the higher pressure (60psi -  $We = 2.16$ ) scenario as the droplets impacted the dry surface, while no prompt splash (no microdroplets observed in frame) was witnessed for any of the lower pressure (0psi -  $We = 0.54$ ) scenario droplet impacts. This is in line with the expectation that increased pressure would potentially influence the droplet splash dynamics.

# Chapter 4

## 4 Conclusions

We can conclude and confirm that there is a significant correlation between higher ambient pressure (leading to higher aerodynamic forces and Weber number), average droplet oblate shape (higher aspect ratio) and increased amplitude of droplet shape oscillations prior to impact.

For conditions where droplet splash was expected on the dry surface due to influence by increased ambient pressure, the droplet shape prior to impact was expected to, most likely, be oblate in shape and experiencing significant droplet shape oscillations and internal circulation. This shape phenomenon was likely due to increased air density and aerodynamic forces affecting the droplet as it descends, which can be characterized by a higher aerodynamic Weber number,  $We \gg 1$ .

With regards to droplet shape and average aspect ratio specifically, our study was able to explicitly show a correlation between higher aerodynamic Weber number and higher average aspect ratio (or transition to an oblate shape from spherical on average) in Table 3.2. With that correlation we can conclude that, in previous studies that also varied ambient pressure for droplets descending prior to impact, the average shape of droplets on impact had a relatively high likelihood of being oblate. Considering other previous studies showing that droplet shape, on impact, does have an effect on the dynamics of lamella spreading and the onset of splash, the average oblate droplet shape may be a contributing factor to the onset of splashing that has been witnessed in previous ambient pressure studies (as well as this study) when the ambient pressure, velocity (and subsequent Weber number) get high enough.

Beyond the average oblate shape of the droplets prior to impact at higher Weber numbers, our results also showed shape volatility in the droplets (also in line with expectations) in Table 3.3. The higher fluctuation in the deviation from an aspect ratio of 1 in the higher pressure scenario implies that there may be some internal dynamics of droplets, during their descent that may have an influence on the likelihood of splash. However, further studies investigating fluctuation magnitude of droplets subject to higher drag and measurements of those modes compared to potential splash dynamics would need to occur to determine if the correlation

between droplet oscillation fluctuations (or droplet shape volatility) and higher drag have any influence on influencing splash upon impact on a dry surface.

Additionally, the majority of previous studies experimentally investigating ambient pressure effects on droplet impact on a dry surface were performed under partial vacuum. The results within this current study can help to serve as confirmation that partial vacuum, itself, was not entirely the driving factor in reducing splash. The properties of the surrounding air, most likely air density, and subsequent increase in drag may be inducing droplet dynamics that are promoting the splash. This helps to verify the theory that the droplet splash is likely a result of aerodynamic forces acting on the fast-spreading lamella upon droplet impact.

#### 4.1 Significance of Findings

In general, the significance of these findings are that, increasing ambient pressure with water droplets impacting a dry surface does influence the incidence of prompt splash. For any applications, industries or studies that involve droplets impacting a dry surface in variable ambient pressure environments (e.g. spray cooling, combustion or pressurized droplet based printing), this phenomenon could be something included in the design considerations for the droplet systems involved in those fields.

Additional significance is that, for future experimental and numerical studies investigating ambient pressure effects on droplet impacts, there may be a need consider droplet shape and droplet oscillations in the analysis.

Following the discovery that ambient pressure significantly influences the onset of splash from a droplet impacting a dry surface by Xu et al in 2005 [1], several studies followed that attempted to help explain the phenomenon. Many of these studies were numerical studies that utilized computational fluid dynamics and simulations to attempt to duplicate the affect seen experimentally [2] [26] [24] [36]. There was some success in this, however, there were still some significant differences in the experimental results compared top the numerical ones. One source of these discrepancies may be a lack of shape consideration in the numerical studies. The majority of numerical studies investigated 2-dimensional, non-oscillating (i.e. no internal circulation) and circular (representing a spherical drop). The results of this current study shows that there is a high likelihood that droplets impacting a dry surface and producing a splash would be oblate in shape

(high aspect ratio), have a dimple depression in the bottom of the droplet and be experiencing relatively high, potentially non-periodic shape oscillations and internal circulation.

## 4.2 Future Work

Considering the range of applications that may benefit from the type of research presented here, there is a large range of specific studies that may help for each particular application. This leads to several potential studies that are more application specific.

In more general terms, there is also a lot of future work that may be able to help with the general clarity of understanding of the droplet shape influence on dry surface splash in varying ambient pressure environments.

The following is a short list of some potential future works that may be able to follow from the results and analysis of this study:

- 1) Acquire more data to help establish a splashing threshold. A larger range of droplet velocities, ambient pressures and droplet properties could be investigated to gain a higher resolution understanding of the phenomena, when they occur and relate them to potential parameters that could be developed to better predict when droplet splash on a dry surface can be expected.
- 2) Acquire more, higher resolution data on droplet shape and influence on prompt splash. The current study included data acquisition with video at 20,000 frames per second and a spatial resolution of about 50 micrometers. Considering the extremely small timeline for the prompt splash phenomenon and the expulsion of secondary droplets that can be smaller than 50 micrometers, a higher temporal and spatial resolution study could greatly improve the understanding of the phenomena.
- 3) Acquire more data on the onset and modes of internal circulation on droplets as they descend in various ambient pressure conditions (potentially by utilizing particle image velocimetry techniques) and assess the potential for internal circulation affect on average droplet shape and potential influence on splash dynamics.
- 4) Perform numerical studies that more accurately match the likely shape of the droplet on impact (with the dimple) and include internal circulation in the descending droplet prior to impacting the dry surface.

## Bibliography

- [1] L. Xu, W. W. Zhang and S. R. Nagel, "Drop splashing on a dry smooth surface.," *Physical review letters*, vol. 94, no. 18, p. 184505.1–184505.4, 2005.
- [2] Y. Guo, Y. Lian and M. Sussman, "Investigation of drop impact on dry and wet surfaces with consideration of surrounding air.," *Physics of Fluids*, vol. 28, no. 7, 2016.
- [3] A. Latka, A. Strandburg-Peshkin, M. M. Driscoll, C. S. Stevens and S. R. Nagel, "Creation of prompt and thin-sheet splashing by varying surface roughness or increasing air pressure.," *Physical review letters*, vol. 109, no. 5, p. 054501–054501, 2012.
- [4] B. R. Mitchell, T. E. Bate, J. C. Klewicki, Y. P. Korkolis and B. L. Kinsey, "Experimental Investigation of Droplet Impact on Metal Surfaces in Reduced Ambient Pressure.," *Procedia manufacturing*, vol. 10, p. 730–736, 2017.
- [5] A. L. Yarin, "Drop impact dynamics: Splashing, spreading, receding, bouncing.," *Annual Review Fluid Mechanics*, vol. 38, p. 159, 2006.
- [6] R. F. Allen, "The role of surface tension in splashing," *Journal of colloid and interface science*, vol. 51, no. 2, pp. 350-351, 1975.
- [7] H. E. Edgerton and J. R. Killian, *flash! Seeing the unseen by ultra high-speed photography*, Boston, MA: Charles T Branford Company, 1954.
- [8] A. M. Worthington, *A Study of Splashes*, London: Longmans Green & Co, 1908.
- [9] C. Mundo, M. Sommerfeld and C. Tropea, "Droplet-wall collisions: Experimental studies of the deformation and breakup process.," *International journal of multiphase flow*, vol. 21, no. 2, p. 151–173, 1995.
- [10] L. Rayleigh, "On the Capillary Phenomena of Jets.," *Proceedings of the Royal Society of London*, vol. 29, pp. 71-97, 1879.
- [11] E. Loth, "Quasi-steady shape and drag of deformable bubbles and drops.," *International journal of multiphase flow*, vol. 34, no. 6, p. 523–546, 2006.
- [12] Z. Xu, L. Wang, T. Wang and Z. Che, "Crown rupture during droplet impact on a dry smooth surface at increased pressure.," *Physics of fluids*, vol. 33, no. 12, 2021.
- [13] E. H. Luo, "Fundamental research and application of droplet dynamics.," in *IntechOpen*, London, 2022.

- [14] Y. Lin and J. Palmore, "Effect of droplet deformation and internal circulation on drag coefficient.," *Physical review fluids*, vol. 7, no. 12, 2022.
- [15] G. Riboux and J. M. Gordillo, "Experiments of drops impacting a smooth solid surface: A model of the critical impact speed for drop splashing.," *Phys. Rev. Lett.*, vol. 113, p. 024507, 2014.
- [16] Y. Liu, P. Tan and L. Xu, "Kelvin–Helmholtz instability in an ultrathin air film causes drop splashing on smooth surfaces.," *Proc. Natl. Acad. Sci. U. S. A.* 112, p. 3280–3284, 2015.
- [17] L. Xu, L. Barcos and S. R. Nagel, "Splashing of liquids: Interplay of surface roughness with surrounding gas.," *Physical review. E, Statistical, nonlinear, and soft matter physics*, vol. 76, no. 6 Part 2, p. 066311–066311, 2007.
- [18] Q. Liu, J. H. Y. Lo, Y. Liu, Y. Li, J. Zhao and L. Xu, "The role of drop shape in impact and splash.," *Nature communications*, vol. 12, no. 1, p. 3068–3068, 2021.
- [19] J. E. Sprittles, "Kinetic effects in dynamic wetting.," *Phys. Rev. Lett.* 118, p. 114502, 2017.
- [20] H. Cheng and C. Lin, "The morphological visualization of the water in vacuum cooling and freezing process.," *Journal of food engineering*, vol. 78, no. 2, p. 569–576, 2007.
- [21] K. V. Beard, V. N. Bringi and M. Thurai, "A new understanding of raindrop shape.," *Atmospheric research*, vol. 97, no. 4, p. 396–415, 2010.
- [22] R. A. van der Veen, T. Tran, D. Lohse and C. Sun, "Direct measurements of air layer profiles under impacting droplets using high-speed color interferometry.," *Physical review. E, Statistical, nonlinear, and soft matter physics*, vol. 85, no. 2 Part 2, p. 026315–026315, 2012.
- [23] W. Bouwhuis, R. A. van der Veen, T. Tran, D. Keij, D. L. Winkels, K. G. Peters, I. R. van der Meer, D. Sun, C. Snoeijer, J. H and D. Lohse, "Maximal air bubble entrainment at liquid-drop impact.," *Physical review letters*, vol. 109, no. 26, p. 264501–264501, 2012.
- [24] A. P. Boelens, A. Latka and J. J. de Pablo, "Observation of the pressure effect in simulations of droplets splashing on a dry surface.," *Physical review fluids*, vol. 3, no. 6, 2018.
- [25] M. Ebrahim and A. Ortega, "Identification of the impact regimes of a liquid droplet propelled by a gas stream impinging onto a dry surface at moderate to high Weber number.," *Experimental thermal and fluid science*, vol. 80, p. 168–180, 2017.
- [26] W. Xiong and P. Cheng, "3D lattice Boltzmann simulation for a saturated liquid droplet at low Ohnesorge numbers impact and breakup on a solid surface surrounded by a saturated vapor.," *Computers and Fluids*, vol. 168, p. 130–143, 2018.

- [27] M. Pilch and C. A. Erdam, "Use of breakup time data and velocity history data to predict the maximum size of stable fragments for acceleration-induced breakup of a liquid drop.," *International journal of multiphase flow*, vol. 13, no. 6, p. 741–757, 1987.
- [28] F. Hansen and G. Rødsrud, "Surface tension by pendant drop: I. A fast standard instrument using computer image analysis.," *Journal of colloid and interface science*, vol. 141, no. 1, pp. 1-9, 1991.
- [29] M. Fukumoto, K. Yang, K. Tanaka, T. Usami, T. Yasui and M. Yamada, "Effect of Substrate Temperature and Ambient Pressure on Heat Transfer at Interface Between Molten Droplet and Substrate Surface.," *Journal of Thermal Spray Technology*, Vols. 20(1-2), p. 48–58, 2011.
- [30] B. Zhang, Y. Ling, P. H. Tsai, A. B. Wang, S. Popinet and S. Zaleski, "Shortterm oscillation and falling dynamics for a water drop dripping in quiescent air.," *Physical review fluids*, vol. 4, no. 12, 2020.
- [31] J. N. Fannesbeck, "Release of Large Water Droplets.," All Graduate Theses and Dissertations, <https://digitalcommons.usu.edu/etd/8443>, Utah State University, 2022.
- [32] V. Serdyukov, N. Miskiv and A. Surtaev, "The Simultaneous Analysis of Droplets' Impacts and Heat Transfer during Water Spray Cooling Using a Transparent Heater.," *Water (Basel)*, vol. 13, no. 19, p. 2730, 2021.
- [33] H. Lamb, *Hydrodynamics*, Cambridge University Press, 1932.
- [34] K. Fahimi, L. Mañdler and N. Ellend, "Measurement of surface tension with freefalling oscillating molten metal droplets: a numerical and experimental investigation.," *Experiments in fluids*, vol. 64, no. 7, 2023.
- [35] E. Becker, W. J. Hiller and T. A. Kowalewski, "Experimental and theoretical investigation of large-amplitude oscillations of liquid droplets.," *Journal of fluid mechanics*, vol. 231, p. 189–210, 1991.
- [36] A. P. Boelens and J. J. de Pablo, "Simulations of splashing high and low viscosity droplets.," *Physics of fluids*, vol. 30, no. 7, 2018.